NASA TECHNICAL MEMORANDUM NASA TM-77461

BALLOON TEST PROJECT

COSMIC RAY ANTIMATTER CALORIMETER (CRAC)

J.C. Christy, G. Dhenain, P. Goret,
J. Jorand, P. Masse, P. Mestreau,
N. Petrou, A. Robin

Translation of "Projet d'Experience Ballon CRAC',
Commissariat A L'energie Atomique, Institut De
Recherche Fondamentale, GIF-SUR-YVETTE, France,
Report DPhG/SAP/83-14R/PhG. April 21, 1983, pp. 1-28.

NATIONAL AERONAUTICS AND SPACE ADMINISTRATION
WASHINGTON, D.C. 20546 JANUARY 1984

STANDARD TITLE PAGE

1. Report No. NASA TM-77461	2. Government Accession No.	3. Recipient's Catalog No.
4. Title and Subtitle BALOON TEST PROJECT - COSMIC RAY ANTIMATTER CALORIMETER (CRAC)		5. Report Date January 1984
		6. Performing Organization Code
7. Author(s) J.C. Christy, G. Dhenain, P. Goret, J. Jorand, P. Masse, P. Mestreau, n. Petrou, A. Robin		8. Performing Organization Report No.
		10. Work Unit No.
9. Performing Organization Name and Address SCITRAN Box 5456 Santa Barbara, CA 93108		11. Contract or Grant No. NASw 3542
		13. Type of Report and Period Covered Translation
12. Sponsoring Agency Name and Address National Aeronautics and Space Administration Washington, D.C. 20546		14. Sponsoring Agency Code

15. Supplementary Notes

Translation of "Projet d'Experience Ballon CRAC", Commissariat A L'energie Atomique, Institut De Recherche Fondamentale, GIF-SUR-YVETTE, France, Report DPhG/SAP/83-14R/Phg, April 21, 1983, pp. 1-28

16. Abstract

The CRAC experiment will attempt to measure the flux of anti-matter in the 200-600 Mev/m energy range and the isotopes of light elements between 600 and 1000 Mev/m. Balloon flights will be made in Canada in 1986.

17. Key Words (Selected by Author(s))	18. Distribution Statement UNLIMITED U.S. Government Agencies only		
19. Security Classif. (of this report) Unclassified	20. Security Classif. (of this page) Unclassified	21. No. of Pages 30	22. Price

BALLOON TEST PROJECT
COSMIC RAY ANTIMATTER CALORIMETER (CRAC)

J.C. Christy, G. Dhenain, P. Goret, J. Jorrand,
P. Masse, P. Mestreau, N. Petrou, A. Robin
Astrophysics Service (CEN-Saclay)

I - INTRODUCTION

/1*

The presence of antimatter in galactic cosmic radiation was recently established (1), (2), (3). The table below summarizes the characteristics of these three experiments.

Ref.	Energy (Gev/n)	Geometr. Factor (cm2.sr)	# of $\bar{p}$ detected	Type of detector	$\bar{p}/p$ measured
(1)	3 - 6	200	30	Magnet	5×10^{-4}
(2)	2 - 5	1	2	Magnet	6×10^{-4}
(3)	< .3	120	14	Calori-meter	2×10^{-4}

Figure 1 shows the $\bar{p}/p$ ratios measured as a function of energy. The curves correspond to the predictions of the various cosmic radiation propagation models in the galaxy, on the hypothesis that there is no primary antimatter component. We see that the two high-energy measurements are fairly close to the predictions, whereas the low energy point is on several orders of magnitude above the expected value. This result could indicate the presence of a primary antiproton component. Yet, this conclusion remains very hypothetical for two reasons:

i-the detection method used for low energy conditions renders the result very uncertain;

ii-not a single antihelium nucleus has been detected yet ($\bar{He}/He < 2 \times 10^{-5}$ according to ref. (3)).

*Numbers in the margin indicate pagination in the original text.

Another explanation recently suggested concerns the $\bar{n}$-n oscillation predicted by the theories of high unification (4). The purpose of the CRAC experiment is to measure the flux of anti- /2 matter ($\bar{p}$ and $\overline{He}$) in the 200-600 Mev/n energy range with the following characteristics:

-a high geometric factor (420 cm2.sr)
-a high detection sensitivity
-the presence of contamination due to spurious events $<10^6$

These three factors combined should make it possible to detect antimatter at the $\bar{p}/p=10^{-4}$ level.

No other experiment on antimatter in cosmic radiation is being considered by other laboratories.

The second objective of the CRAC experiment is to measure the isotopes of light elements ($Z<8$) between 600 and 1000 Mev/n. The measurements performed until present pertained to low energy (<150 Mev/n) and their interpretation is obscured by i) solar modulation which is very substantial at low energy and ii) our inadequate knowledge of the effective sections which also vary rapidly with energy. The measurement proposed here overcomes these shortcomings for the most part. The scientific benefit of these isotopic measurements is that they make it possible to determine the RC trajectory distribution in the galaxy corresponding to the longest trajectories.

II - $\bar{p}$ Detection Principle

When an antimatter nucleus interacts with ordinary matter, this causes annihilation associated with the emission of secondary pions. Figure 2 shows a diagram of a $\bar{p}$-p annihilation. On the average, one annihilation produces 3 charge pions (π^+,π^-) and two neutral pions (π°). The π°'s promptly disintegrate into 2γ which may produce a pair (e+,e-), or a Compton electron, due to its interaction with surrounding matter. The energy balance of

The energy balance of the annihilation is:

Available energy	1.9 Gev + kinetic energy
Pion mass	0.7 Gev
Total kinetic energy available for the pions	1.2 Gev + kinetic energy

We thus see that the mean kinetic energy of a pion is about 240 Mev. Figure 3 shows in more detail the energy distribution of the annihilation pions. We thus see that the annihilation products (π,e+e-) are ultrarelativistic particles. We will therefore use a Cerenkov detector to detect the annihilation products. In our case, there is another advantage to using a Cerenkov detector: it is insensitive to slow moving particles. Moreover, as slow moving products are abundant at the time of the nuclear interactions within the Cerenkov itself, the background noise is thus considerably reduced.

III - The Telescope

The telescope proposed is shown in figure 4. It is made up of 2 modules:

-module 1 has 5 functions:

1) to trigger a coincidence signal between T1 and T2

2) to identify the particle charge by means of 6 scintillators T1,T2,S1,S2,S3,S4

3) to measure the flight time between T1 and T2 so as to identify the propagation direction

4) to measure the velocity of the incident particle in the Cerenkov C1

5) to measure the trajectory using a hodoscope S1,S2,S3,S4.

-module 2 is a calorimeter made up of 5 Cerenkov C2 detectors (1 to 5). It is designed to detect the Cerenkov light emitted by the annihilation products.

An anticoincidence protecting module 1 is provided to quickly discard events beyond coincidence .

a- Flight time:

This is the critical point of the experiment. There actually exists a large flux of rising particles either coming from the atmospheric albedo, or from nuclear interactions in the calorimeter. These particles are not only interesting, but are also capable of simulating an antiproton signal, if necessary. It is therefore necessary to discard these particles with 100% efficiency. In our case, the flight time between the falling particles and the rising particles is < 6 ns. There are actually flight time devices having resolutions on the order of σ=0.2 ns (ref. (5) for example) which would give us a comfortable separation of more than 30 sigmas.

b- The Hodoscope: /4

There are 4 layers (2X and 2Y) of scintillator rods (50x5x3 cm) seen by a PM at each end. The angular resolution is < 2.0 degrees. The advantage of such an hodoscope is its 100% proton efficiency and its relative simplicity. The spatial resolution is amply adequate for correcting the Cerenkov signals of the chart effects which is the main cause of fluctuations. To detect antimatter, the angular resolution is of little significance, the hodoscope being used in this case (excluding determination of the charge) only to contain the events in the calorimeter geometry.

c- Identification of the Charge:

It is well known that scintillators have an excellent resolution for low charge particles which we are concerned with here.

d - Cerenkov Radiators:

The various Cerenkov radiators used in the experiment are all designed according to the same principle. They are made up of a diffusing box filled with a mixture of purified water & shifter (2-amino-6 acid di-potassium salt, disulfonic 8-napthtalene abbreviated amino-G salt). The boxes are round with dimensions ϕ=80 cm - h=20 cm for the 5 Cerenkov of the calorimeter and ϕ=60cm - h=15 cm for the C1 Cerenkov. The water in each box is seen directly by 12 PM, the PM window being in contact with the water. We thus gain a factor on the order of 3 to 4 on the number of photoelectrons with respect to a PM viewing the water through a transparent window. Numerous Cerenkov with water+shifter were used in in the pass (6),(7). The addition of shifter has a dual effect on the primary Cerenkov light: i) the UV radiation which is more significant is absorbed by the shifter and reemitted at 400 nm, i.e. in the photocathode efficiency peak and ii) the re-emission is isotropic which effaces the directivity of the primary emission. We thus gain a factor of about 4 on the number of photoelectrons by adding the shifter. Furthermore, an interesting property of water is the absence of scintillation, as shown in figure 5. The water ahs a refraction index of n=1.33 which gives an energy threshold of 480 Mev/n.

Based on the existing data on the Cerenkov with water, we may estimate the number of photoelectrons which may reach radiators such as those proposed here. The parameter which interests us is the number of photoelectrons collected per cm of water for a charge particle Z=1 and velocity v/c=1. This parameter is shown in figure 6 as it is measured in the reference (6) as a function of the ratio of photocathode surface to the total internal surface of the radiator s-S(PM)/(total)S. We have also shown in this figure the number s corresponding to our radiators. We see that the C1 Cerenkov could collect 38 p.e/cm and the calorimeter Cerenkovs 25 p.e/cm.

Utilization of the Cerenkov water radiators thus appears to be quite appropriate for our present needs. One particle which passes the T1-T2 coincidence will trigger C1 or otherwise. depending on whether its kinetic energy per nucleon is less or not than the threshold energy of 480 Mev/n. The particle then penetrates into the calorimeter while decelerating. If the particle is a proton it will give a calorimeter signal which is definitely lower than the C1 signal. Conversely, an antiparticle will become annihilated in the calorimeter by producing a signal which is much higher than the C1 signal. We will note that the antiparticles may become annihilated in flight or at rest after the deceleration. This fact affects the characteristics of the antimatter signal only very slightly.

IV - Simulation of the Experiment

A simulation of the annihilation process was performed by Monte-Carlo for the purpose of studying the telescope performances. The simulation program handles:

-the effective annihilation section of the $\bar{p}$'s in matter in the telescope. This effective section is parametrized by: $\sigma=48A^{1/3}\ \beta^{-.868}$ A=target mass and $\beta=v/c$. In figure 7 we see a comparison between this formula and the experimental results.

-multiplicity of the annihilation pions (see figure 8).

-the energy distribution of the annihilation pions (figure 3).

-the instaneous disintegration of the π° into 2γ.

-the interaction of the γ in the calorimeter producing a Compton e or an e^+, e^- pair.

The annihilation pions are isotropically generated in the center of mass, their direction and their energy being restored in the laboratory system by means of the Lorentz transform. The distribution of the pions in time is generated by the GENEV subprogram borrowed from the CERN-LIBRARY W-505. For illustration,

we show in figure 9 the distribution of the effective masses π^+ π^+ and π^- π^- in the $\bar{p}$-p annihilation at rest. The secondary particles emitted at the time of the annihilation are followed in the various detectors with integration of the Cerenkov light. At the time of an annihilation in flight, the number of pions emitted is appreciably the same as for an annihilation at rest: only their kinetic energy increases. Figure 10 shows the distribution of the antiproton signals in the calorimeter, on the pessimistic assumption that the calorimeter efficiency is 15 p.e/cm. The distribution width reflects the fact that certain secondary annihilation particles may escape from the calorimeter. We therefore see that the annihilation of a p typically produces several thousands of photoelectrons. By comparison, a proton of velocity v/c=1 passing through the calorimeter would produce about 1500 p.e (it would of course discard $\bar{p}$ as a candidate by the high signal it would produce in C1). The upper energy limit of the telescope is about 600 Mev/n which corresponds to the energy of a $\bar{p}$ (or a p) which is totally decelerated in the calorimeter. The maximum light emitted by a particle in the calorimeter would be achieved for a Deuterium of 600 Mev/n which would produce about 60 p.e in C2, or 25 times less than the mean antiproton signal. The antihelium signal will be 4 times the $\bar{p}$ signal, i.e. an average of about 6000 p.e.

The antimatter detection efficiency is determined by 2 factors:

-the proportion of antiparticles which become annihilated in module 1;

-the proportion of antiparticles which become annihilated in the calorimeter, but one or several of whose secondary products rise in module 1.

In the 2 cases, the signals of the various detectors of module 1 will very probably be inconsistent and the event will be discarded. In figure 11 we showed the telescope efficiency of the $\bar{p}$'s calculated by the simulation program. The efficiency is lower

for i) the probability of annihilation in module 1 is greater and ii) the annihilation point in the calorimeter is closer to module 1 and therefore the probability of having a secondary ascendant is greater. The 2cm thick lead plate is used to absorb part of the ascendants, the electrons in particular. /7

In conclusion, the efficiency between 200 and 480 Mev/n is 28%, it is therefore 53% between 480 and 600 Mev/n.

V - Background Noise

We may consider various causes capable of simulating an anti-proton event (the problem is much less critical in the case of He).

1 - The nuclear interactions in the calorimeter: the interaction products are either slow nuclei (whose energy is quite a bit lower than the Cerenkov threshold of water), or pions. The production threshold of relativistic pions in a p-p or p-n reaction is about 600 Mev. The energy of the particles in the calorimeter being less than 600 Mev/n, the nuclear interaction pions cannot give a large signal in C2.

2 - The diffusion of particles in a calorimeter PM. In this case only one PM would be affected, in contrast to the p signal where several PMs are affected. The Cerenkov radiators of the calorimeter are analyzed by 2 distinct channels corresponding to 2 half-rings (1 PM in 2). We may thus discard the events where a single half-ring produces a signal.

3 - The $\bar{p}$'s of atmospheric origin: 5g/cm2 of residual atmosphere, the p flux produced by the interaction of the cosmic radiation with the atmosphere is $\bar{p}/p << 10^{7}$ at low energy. This is due to the fact that the probability of producing an energy p < 1 Gev is extremely small.

4 - Random coincidences: let us assume that during the the acquisition system analyzes a proton event, the relativistic particle passes through the calorimeter without passing through the coincidence. This particle would produce a fairly large quantity of light in C2 to simulate an antiproton signal. We may estimate the flux of relativistic particles passing through C2 to be $\phi=5\times10^{3}$ p/sec. For a typical dead time of $\tau=3\mu$sec the probability of random coincidence is:

$$Pc= (\phi\tau)^{2}/2=10^{-4} \qquad /8$$

Our objective being to achieve a sensitivity of 10^{-4}, we see that the rate of random coincidences might contaminate the measurement of the $\bar{p}/p$ ratio (although not all random coincidences can simulate an antiproton event).

The CRAC experiment will be equipped with a system for discarding random coincidences. We will use a rapid monitoring channel designed to measure the time separating the arrival of two successive calorimeter pulses (analogous to an anti-pile up system used on an accelerator).

VI - Telescope Performances

VI.I - Antimatter

Geometric Factor = 420 cm2.sr
Half-angle of opening of telescope = 12 degrees

Energy (Mev/n)	Proton Flux (p/sec)	Telescope Efficiency	a p p Sensitivity (/hour)
200-480	24	0.28	4×10^{-5}
480-600	8	0.53	6×10^{-5}

We thus see that with a balloon flight of about thirty per hour, we achieve a sensitivity of about 8×10^{-7} in the determination of the $\bar{p}/p$ ratio. The sensitivity at the $\overline{He}$ is not as satisfactory, because the $\overline{He}$ interactions in module 1 will be greater and the mean number of secondary ascendants will be 4 times higher than for the $\bar{p}$'s. The telescope efficiency at the He's is 5% and 15% respectively for the low and high energy ranges. This corresponds to a sensitivity of about $1X10^{-5}$ for the measurement of the $\bar{He}/He$ ratio. Conversely, we may consider expanding the energy range to 800-900 Mev/n for the detection of the $\bar{He}$'s, which would then give a sensitivity of about 5×10^{-4}, or one order of magnitude below the current upper limit. The situation for the $\bar{p}/p$ ratio is summarized in figure 12. One should note here that the measured energy range does not correspond to the energy of the cosmic radiuses in the interstellar environment due to the solar /9 modulation. In the table below, we give an estimate of the number of detectable p's for 2 solar modulation conditions and a flight of 30 hours.

		-----presumed model-----		
Solar Activity	Energy loss in the solar cavity (Mev)	primary $\bar{p}$ ref. (3)	closed galaxy	leaky box
Minimum	300	210 p	11 p	2 p
Maximum	600	40 p	6 p	1 p

VI.II - Isotopes

The CRAC telescope can separate the isotopes from the cosmic radiation in an energy range from 600 to 1000 Mev/n. The detection principle is the following: a particle which triggers the Cerenkov C1 penetrates into the calorimeter C2 where it undergoes an energy loss per nucleon which is dependent upon the ratio Z^2/A (Z-charge, A=mass). In the calorimeter, the particle will emit Cerenkov light as long as its energy level is greater than 480 Mev/n.

Therefore, for an equal signal in C1, a heavy particle will give a greater C2 signal than that of a lighter particle. In figure 13 we see the C2 signal as a function of the C1 signal for hydrogen and deuterium. Figure 14 shows the mass spectra for the preceding figure: the mass resolution is on the order of 0.12 mass unity. In this estimate, no correction was made of the angle of incidence ($0<\theta<12$ degrees) which would improve the resolution even more.

VII - Specifications

The CRAC experiment is planned to be launched by balloon. The telescope will be inside a pressurized pod. The problem of heat regulation is in large part solved due to the large quantity of water involved in the experiment. The experiment requires the use of 72 PM of photocathodes 120 mm in diameter for the Cerenkov and 80 P.M 37 mm in diameter for the hodoscope. The flight time will be equipped with 8 high-speed PM.

Each Cerenkov and each scintillator layer has its own high- /10
voltage power supply, i.e. 10 HV power supplies plus one HV for the flight time.

Each hodoscope PM has its own analysis channel. Conversely, each Cerenkov only has 2 analysis channels: the 12 PM are assembled in groups of 6 by adding the signals of 1 PM to 2. The Cerenkov will be equipped with square root amplifers (as on HEAO) to accommodate enough dynamics for the isotopic analysis. For the hodoscope signals, one linear amplification is adequate, since the dynamic is only about 100 from Z=1 to Z=8.

A microprocessor on board will have the function of i) sorting the events in real time and ii) adjusting, if necessary, certain test parameters such as thresholds or acceptance criteria. A diagram of the collection system considered is shown in figure 15. The Ranging rates is estimated at 20-30 kbits/sec. We are

also planning to install one (or several) magnetic recorders on board which would serve as a redundancy to the telemetry and which would make it possible to continue the acquisition in the event that the experiment is out of the receiving station's range. Such recorders now exist on the market with a capacity of 65 Moctets for a weight of 2kg.

Telescope Weight

Water	550 kg
Lead	115 kg
Scintillators	40 kg
PM	120 kg
Mechanical	.....
Electronics	.....
Batteries	.....
Pod	.....
Total	1500 kg??

VIII - Implementing the Experiment

The experiment shall be performed in 2 years in the laboratory of the Saclay Astrophysics Service. A calibration of the experiment is planned at an altitude of about 3000 m. The Particles flux at this altitude, although lower than that found in the stratosphere, makes it possible to test a certain number of telescope functions such as anticoincidence and the anti-pile-up /11
system. Furthermore, due to the fact that the antiproton flux is estimated at $p/p=10^{-4}$ at an altitude of 3000m, we can check to what extent the background noise can simulate an antiproton annihilation. Finally, the D/H ratio being on the order of 10^{-3}, we may also measure the isotopic resolution of the experiment in conditions very similar to those of a stratospheric flight.

The telescope will see about $3x10^4$ protons and 30 deutons per day between 400 and 1200 Mev/n. A calibration of some 15 days at an altitude of 3000m should make it possible to become sufficiently familiar with the instrument for a delicate interpretation of the future flight. The calibration data will aslo serve

to develop the analysis programs of the experiment. It would also be desirable to test the antiproton experiment with CERN to verify the parameters established by simulation, efficiency, $\bar{p}$ signal, etc.).

The launching site under consideration is at Fort-Churchill (Canada) where the geomagnetic cut-off is about 200 MV. The optimal period for the launching would be 1986-1987, coinciding with the next lowest solar activity (see figure 16).

The $\bar{p}$ interaction distance in the atmosphere being about 50 g/cm2, it is advantageous to fly at a residual pressure of a few mbars. To achieve this objective, we will use a 750000 m3 balloon.

IX - Implementation Schedule and Financing /12

1983 - Physical, electronics, mechanical studies
Flight Time Completion
Cerenkov 1 Completion
Hodoscope and anticoincidence mock ups

1984 - Hodoscope completion
Calorimeter completion
Beginning of integration and ground testing

1985 - Anticoincidence completion
End of integration and ground testing
Calibration at 3000m altitude
$\bar{p}$ calibration at CERN (if feasible)

1986 - Balloon flights in spring and/or autumn in Canada

BUDGET in thousands of TTC francs

1983 -	
Flight time +Cerenkov 1	150
Data acquisition system	150
	300
1984 -	
5 Cerenkov	400
Mechanics	150
Electronics + Power supply	500
Hodoscope	150
	1200
1985 -	
Mechanics	180
Anticoincidence	120
Missions	50
Recorders	50
	400
1986 -	
Missions+transport (Canada)	250
Batteries	50
	300
Total Cost	2200

REFERENCES

1. R.L. Golden et al., "Phys. Rev. Lett. 43 (1979) p. 1196

2. E.A. Bogolomov et al. Proc.16th Int. Cosmic Ray Conf. Kyoto (1979)

3. A. Buffington et al. Ap. J. 247 (1981) L105

4. J. Arafune and M. Fukugita, 17th Cosmic Ray Conf. Paris 1981 HE-7.6

5. D'Agostini et al. N.I.M. 185 p. 49

6. P. Nemethy et al. N.I.M 173 (1980) p. 251

7. F. Ashton et al. Proc. 11th Int. Conf. Cosmic Rays Budapest (1969) TE-9 p. 27

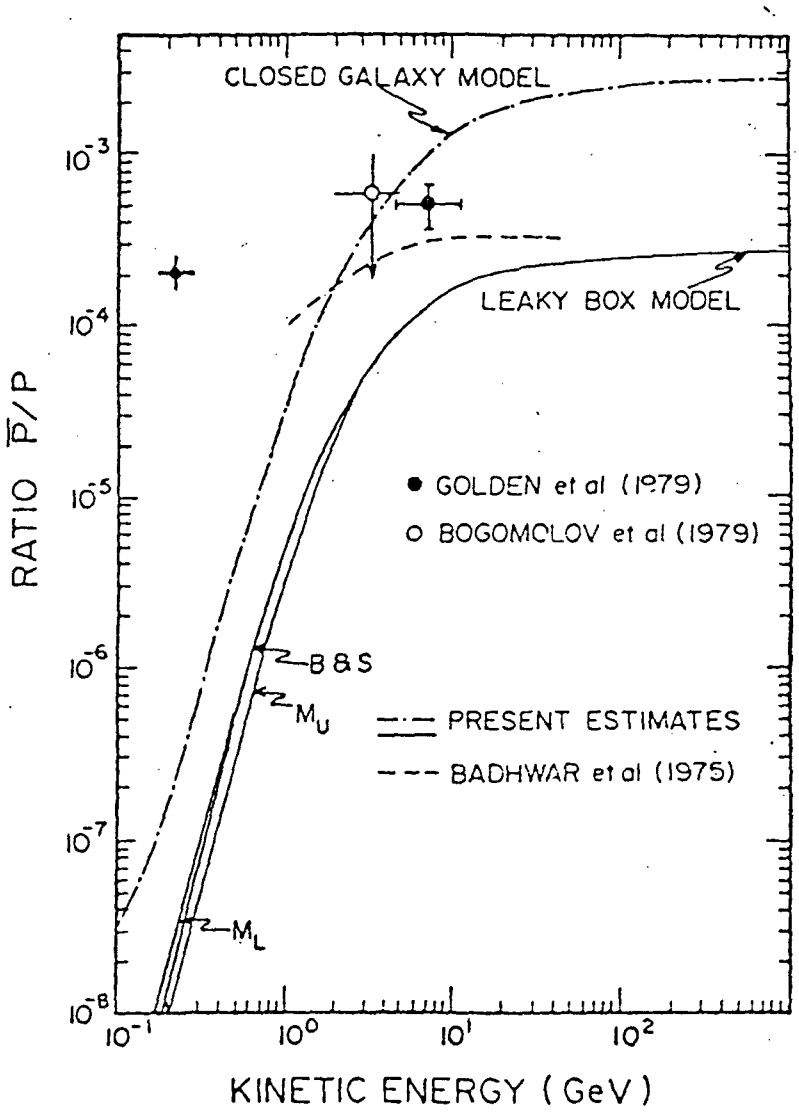

Fig 1. Experimental results on antiprotons. The curves correspond to the various models of radiation propagation in the galaxy.

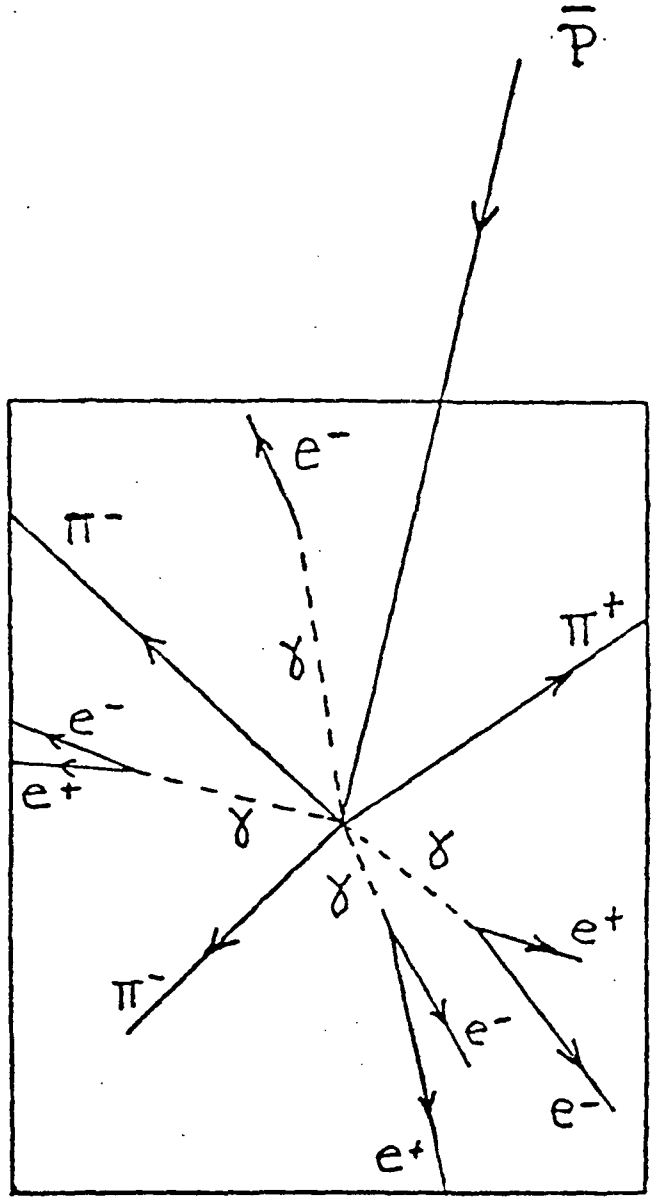

Fig 2. Annihilation of an antiproton with production of charged secondary particles π^+ π^- e^+ e^-

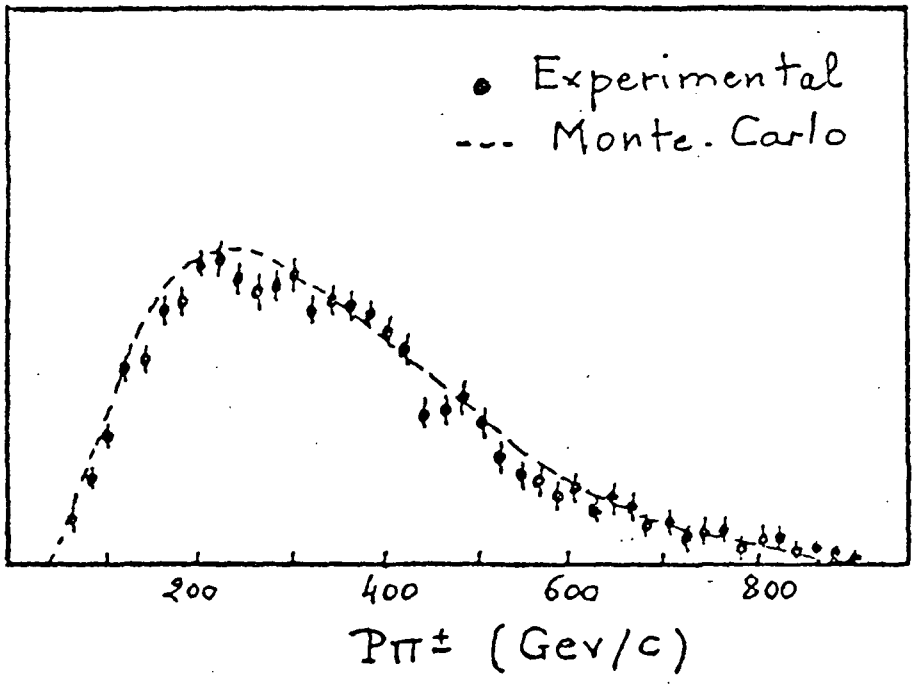

Fig 3. Energy distribution of the annihilation pions.

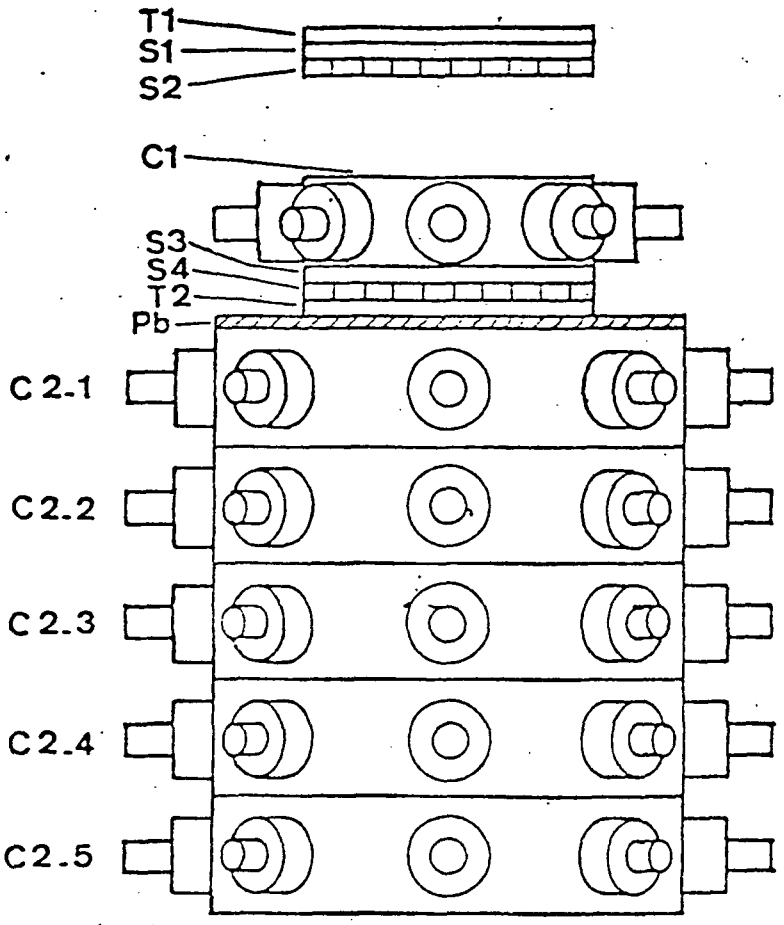

Figure 4 - Diagram of the CRAC telescope

Module 1

T1	TOF+coincidence scintillator ϕ=50 cm h=3 cm
S1	10 scintillator rods X view 50X5X3 cm
S2	ditto, S1, y view
C1	Cerenkov with water ϕ=60 cm h=15 cm
S3	ditto S1 X view
S4	ditto S1 Y view
T2	ditto T1

Calorimeter

C2-1	Cerenkov with water ϕ=80 cm h=20 cm
C2-2	ditto C2-1
C2-3	ditto C2-1
C2-4	ditto C2-1
C2-5	ditto C2-1

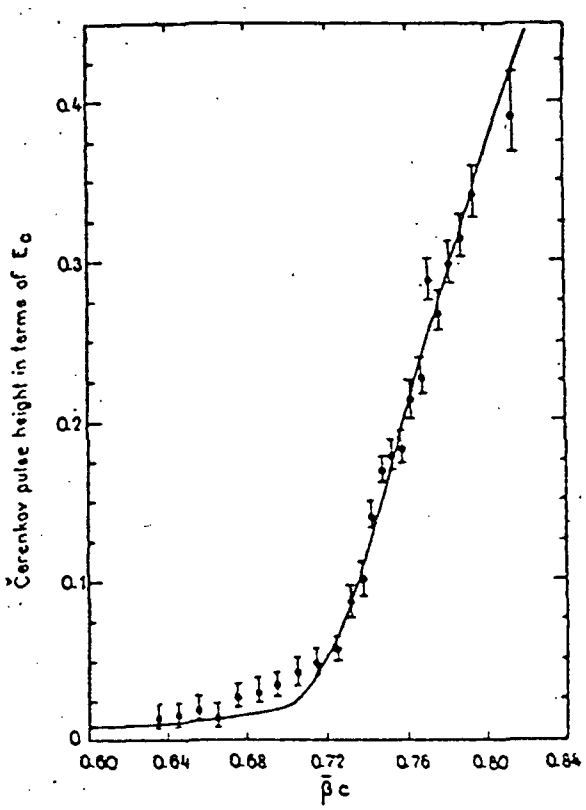

Fig 5. Response of a Cerenkov with water as a function of the particle velocity. The curve represents the expected response without scintillation. The residual light under nominal Cerenkov is due to the δ rays (title of reference (7)).

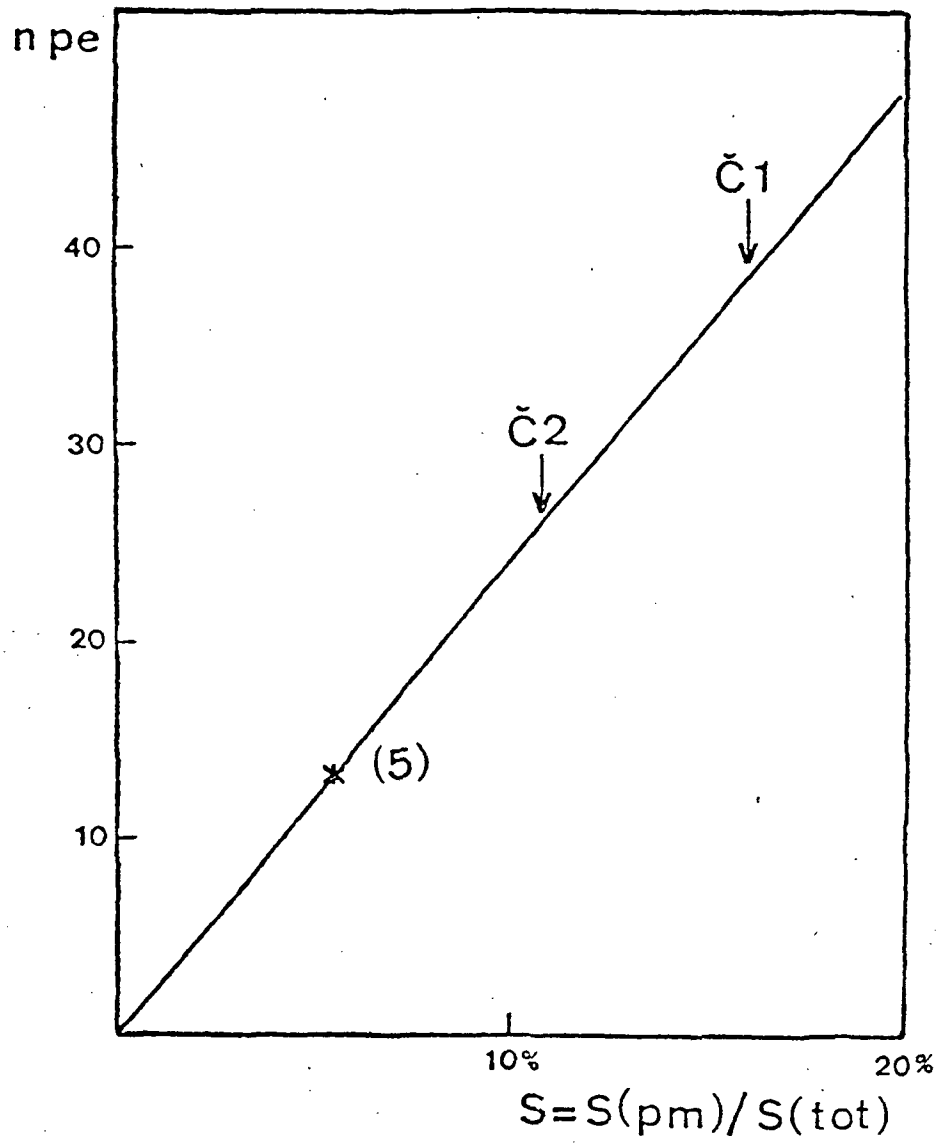

Fig 6. Number of photoelectrons collected per cm of water for a particle Z=1, v/c=1 as a function of the ratio S of photocathode surface to the total internal surface of Cerenkov. The experimental point is taken from reference (6). The ratio S for the CRAC Cerenkov are also shown.

$$\sigma_{ann} = \sigma_o A^{2/3} \beta^{-0.868}$$

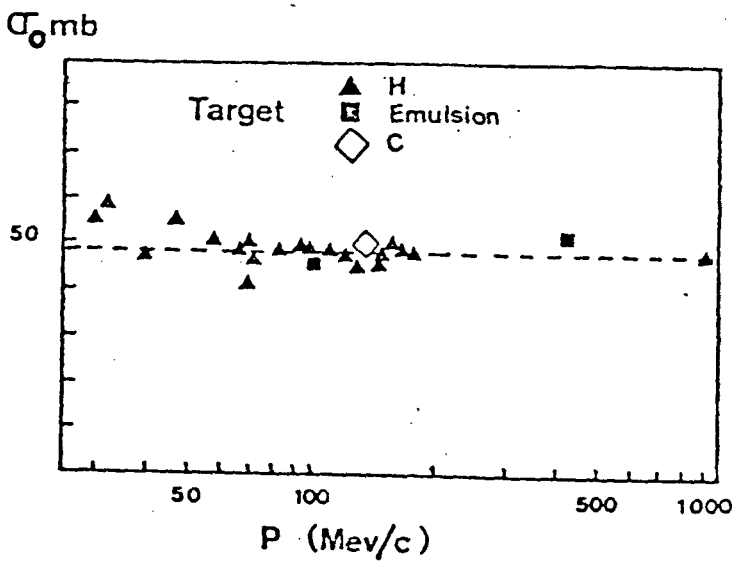

Fig 7. Effective annihilation section of the antiprotons in the various materials.

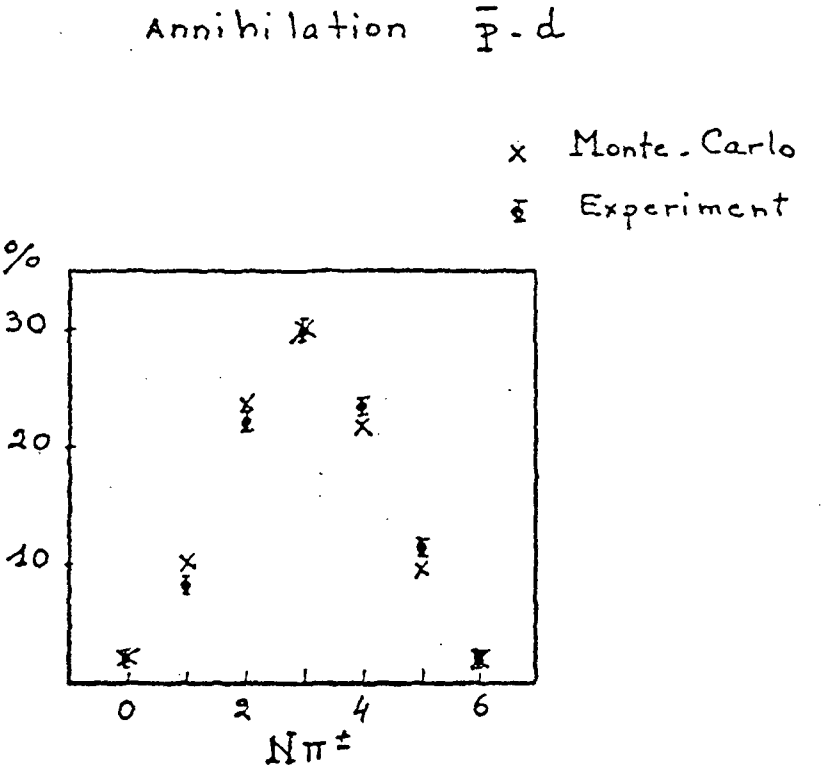

Fig 8. Multiplicity of the pions in the p-p annihilation.

Effective mass of $\pi^+ \pi^+$ and $\pi^- \pi^-$ in the reaction $\bar{p}p \rightarrow \pi^+ \pi^- \pi^\circ$

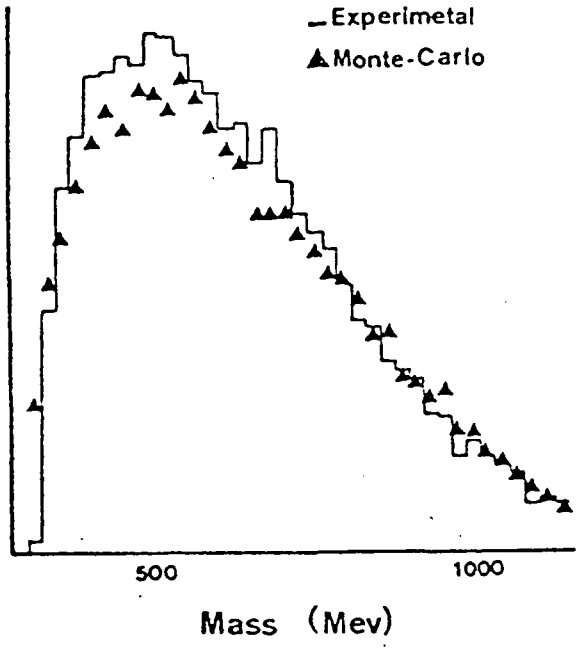

Fig 9. Effective mass of $\pi^+\pi^+$ and $\pi^-\pi^-$ in the $\bar{p}$-p annihilation at rest.

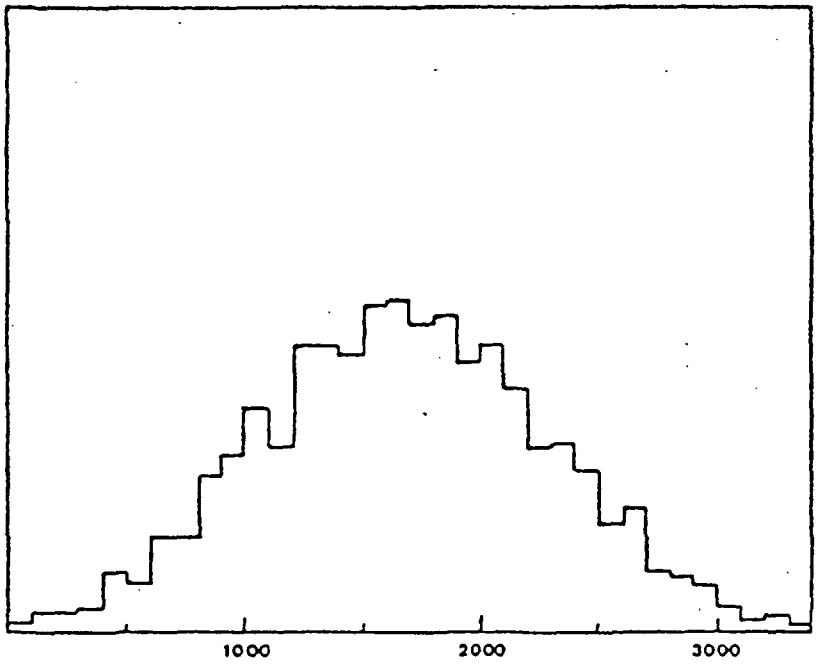

Fig 10. Distribution of the light collected in the calorimeter at the time of $\bar{p}$ annihilation with n=15p.e/cm.

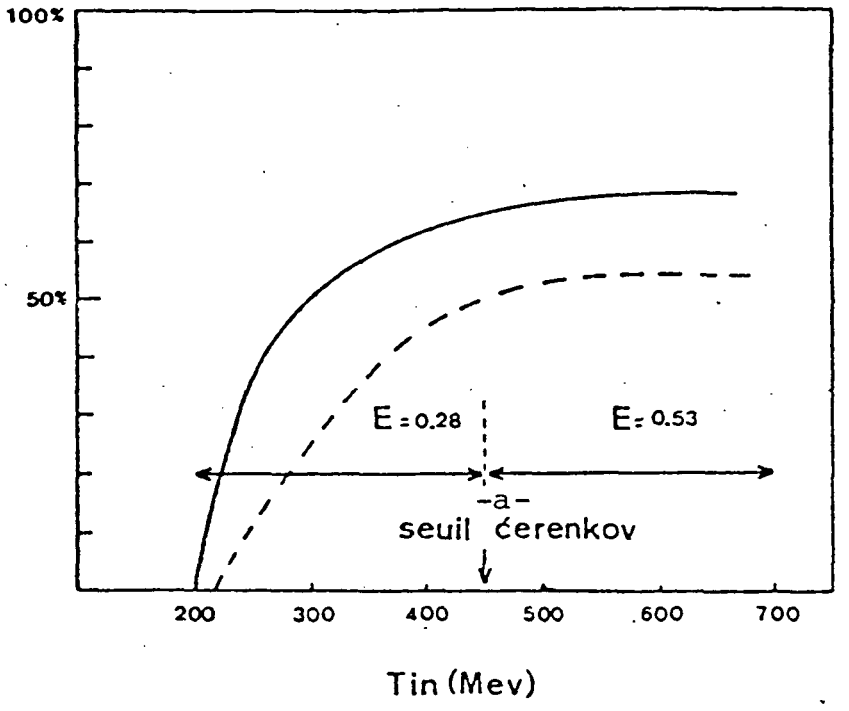

Fig 11. Efficiency of the CRAC telescope for the detection of the $\bar{p}$'s as a function of energy. The full curve represents the fraction of incident $\bar{p}$'s which become annihilated in the calorimeter. The dotted curve gives the fraction of $\bar{p}$'s annihilated in the calorimeter without secondary particles rising in the telescope module.

Key: -a-Cerenkov threshold.

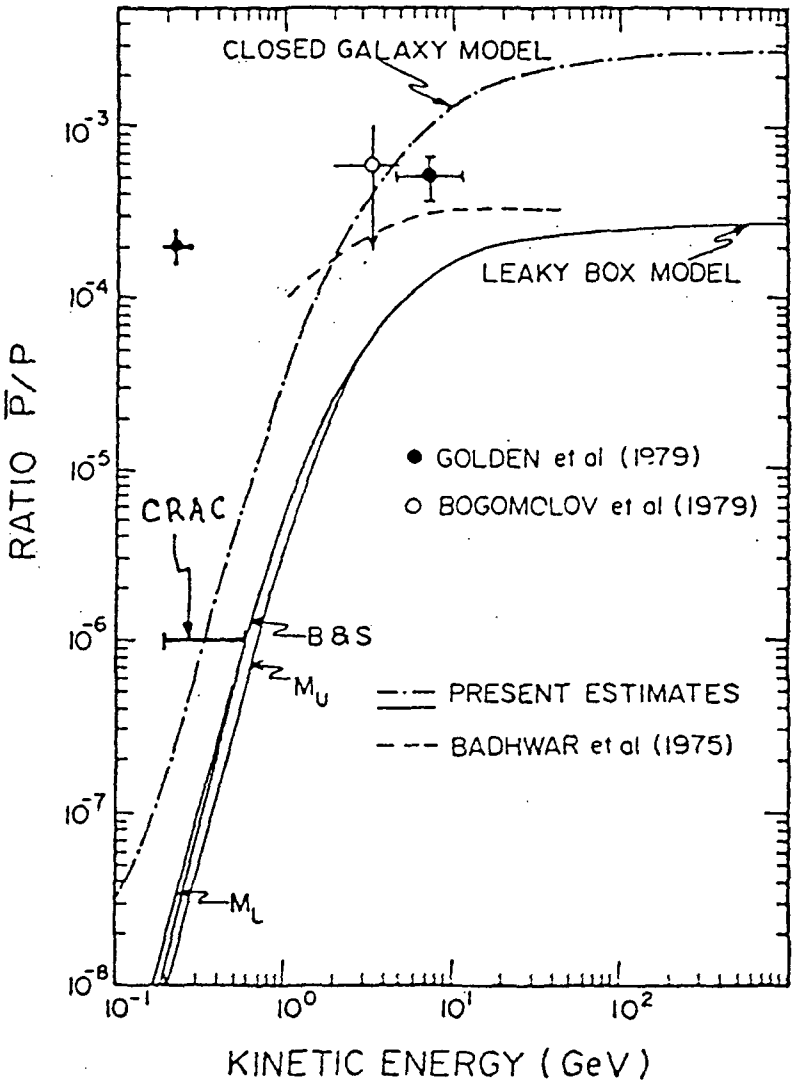

Fig 12-Identical to figure 1. The expected CRAC sensitivity is shown for the $\bar{p}/p$ measurement.

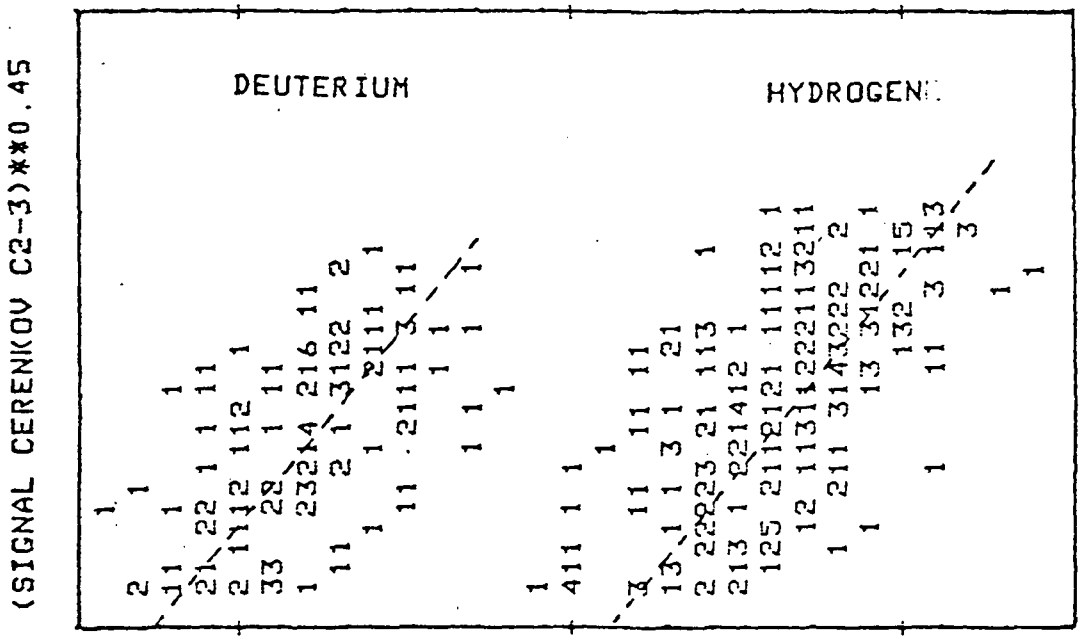

Fig 13-Distribution of the C1 signals versus C2-3 for hydrogen and deuterium between 600 and 700 Mev/n. The calculation was performed with 50 p.e/cm for 2 Cerenkovs.

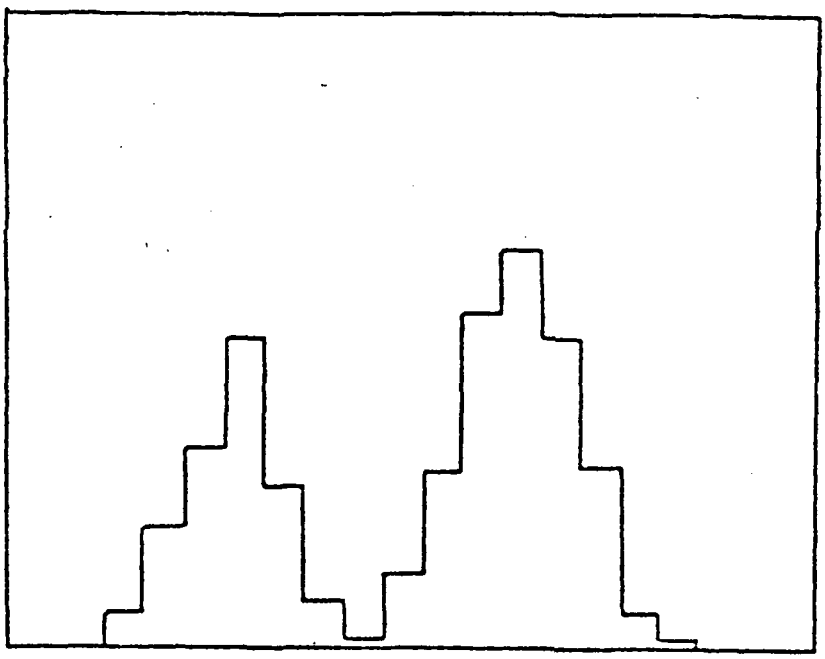

Fig 14-Mass spectrum of H and D obtained by adding the events according to the parallels shown in figure 13. The mass resolution is on the order of 0.12 mass units.

CRAC Electronics

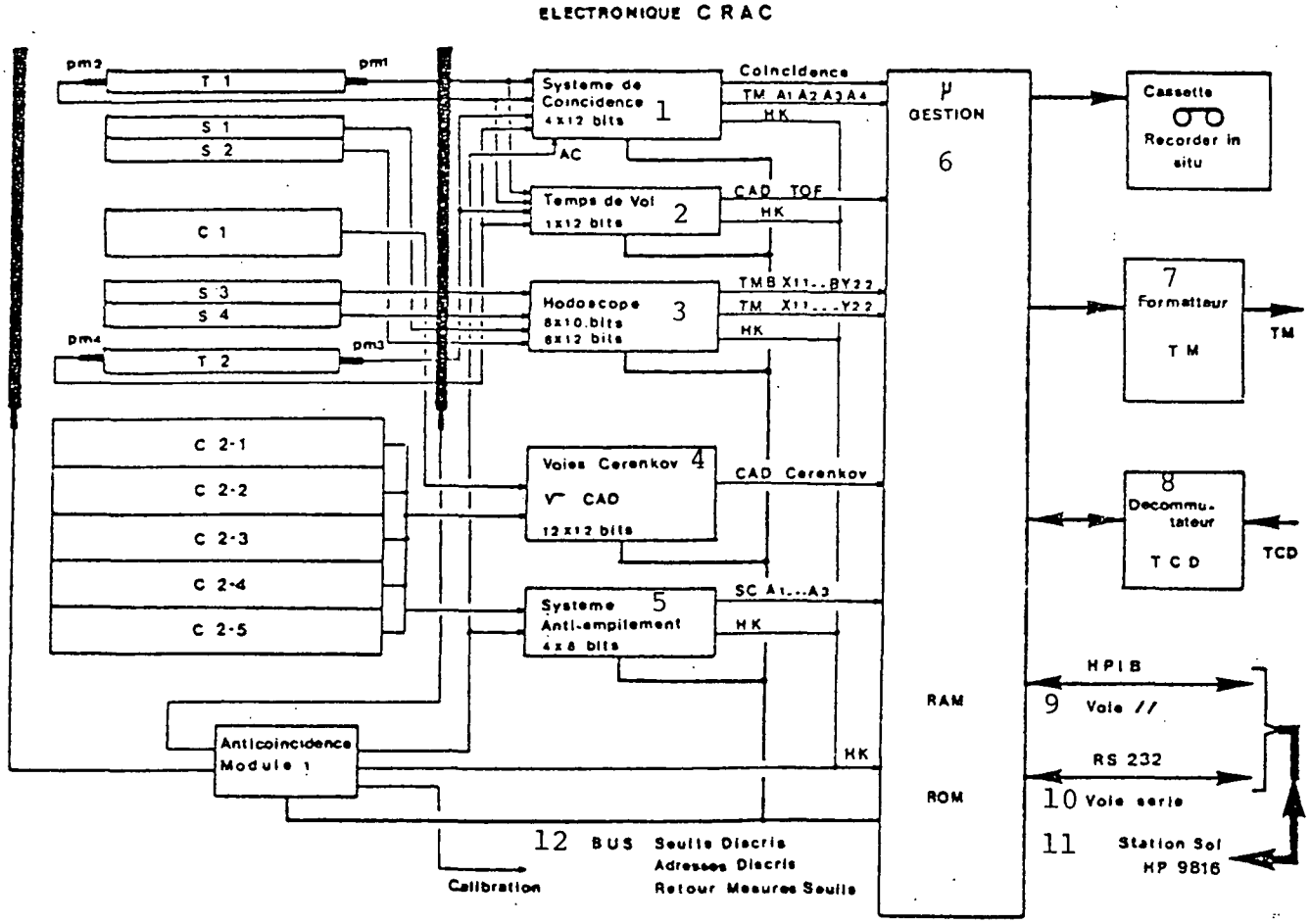

Key: Fig 15-Diagram of the data acquisition system for the CRAC experiment.

1-Coincidence system 4x12 bits; 2-Flight time 1x12 bits; 3-Hodoscope 8x10 bits, 8x12 bits; 4-Cerenkov channels; 5-Anti-stack-up system 4x8 bits; 6-Management; 7-Format device; 8-Unswitching; 9-//Channel; 10-Series channel; 11-Ground station HP 9816; 12-BUS Discris threshold
Discris addresses
Return of threshold measurements.